Mechanics of Materials 40 (2008) 812–824

Contents lists available at ScienceDirect

Mechanics of Materials

journal homepage: www.elsevier.com/locate/mechmat

Variational asymptotic micromechanics modeling of heterogeneous piezoelectric materials

Tian Tang, Wenbin Yu *

Department of Mechanical and Aerospace Engineering, Utah State University, Logan, UT 80322-4130, USA

ARTICLE INFO

Article history:
Received 27 September 2007
Received in revised form 29 April 2008

Keywords:
Piezoelectric heterogeneous materials
Variational asymptotic method
Mircomechanics
VAMUCH

ABSTRACT

In this paper, a new micromechanics model is developed to predict the effective properties and local fields of heterogeneous piezoelectric materials using the variational asymptotic method for unit cell homogenization (VAMUCH), a recently developed micromechanics modeling technique. Starting from the total electric enthalpy of the heterogenous continuum, we formulate the micromechanics model as a constrained minimization problem using the variational asymptotic method. To handle realistic microstructures in engineering applications, we implement this new model using the finite element method. For validation, a few examples are used to demonstrate the application and accuracy of this theory and the companion computer program – VAMUCH.

1. Introduction

Piezoelectric materials such as PZT (Lead, Zirconium, Titanate) are widely used in sensors and actuators due to their property of converting electric energy into mechanical energy, and vice versa. However, bulk piezoelectric materials have several drawbacks for instance their weight, disadvantage of shape control, and acoustic impedance, therefore composite piezoelectric materials are usually a better technical solution in the case of many applications such as ultrasonic imaging, sensors, actuators and damping. Recently, piezoelectric composites are developed by combining piezoelectric materials with passive materials to form a variety of types of piezoelectric composite systems. To facilitate the design of these piezoelectric composites, convenient and accurate analysis tools are apparently indispensable.

In the past several decades, numerous approaches have been proposed to predict the effective properties of piezoelectric composites from known constituent information. Simple analytical approaches based on Voigt or Reuss hypothesis have been applied to predict the behavior of a limited class of composite geometries (Newnham et al., 1978; Banno, 1983; Chan and Unsworth, 1989; Smith and Auld, 1991). Variational bounds have been obtained for describing the complete overall behavior which are useful tools for theoretical consideration (Bisegna and Luciano, 1996, 1997; Li and Dunn, 2001). However the range between bounds can be very large for certain effective properties. Eshelby's solutions (Eshelby, 1957) have been extended to include piezoelectric constituents (Wang, 1992; Benveniste, 1992; Dunn and Taya, 1993b; Chen, 1993). Such mean field-type methods are capable of predicting the entire behavior under arbitrary loads. However, they use averaged representations of the electric and mechanical field within the constituents of the composite, i.e., they do not account for the local fluctuations of the field quantities. This restriction can be overcome by a finite element method-based micromechanical analysis (Gaudenzi, 1997; Poizat and Sester, 1999). In such models the representative unit cell and the boundary conditions are designed to capture a few special load cases which are connected to specific deformation patterns. This allows the prediction of only a few key material parameters. The finite element unit cell models which can capture the entire behavior have recently appeared (Lenglet et al., 2003; Sun et al., 2001; Pettermann and Suresh, 2000; Li,

* Corresponding author. Tel.: +1 435 7978246; fax: +1 435 7972417.
E-mail address: wenbin.yu@usu.edu (W. Yu).

0167-6636/$ - see front matter © 2008 Elsevier Ltd. All rights reserved.
doi:10.1016/j.mechmat.2008.04.007

2000; Pastor, 1997; Berger et al., 2006). Other studies (Dunn and Taya, 1993a, 1994; Huang and Kuo, 1996; Fakri et al., 2003) have focused on the classical extensions of Eshelby's solution for finite inclusion volume fractions, i.e., the Mori–Tanaka (Mori and Tanaka, 1973; Benveniste, 1987) self-consistent approach (Hill, 1965; Budiansky, 1965), differential approaches (McLaughlin, 1977; Norris, 1985), and models based on the generalized Mori–Tanaka and self-consistent approaches (Odegard, 2004).

In this paper, a novel micromechanics model based on the framework of variational asymptotic method for unit cell homogenization (VAMUCH) has been developed to predict the effective properties and local fields of piezoelectric composites. This model invokes two essential assumptions within the concept of micromechanics for composites with an identifiable unit cell (UC):

- *Assumption 1:* The exact field variables have volume average over the UC. For example, if u_i and ϕ are respectively the exact displacements and electric potential within the UC, there exist v_i and ψ such that

$$v_i = \frac{1}{\Omega}\int_\Omega u_i \, d\Omega \equiv \langle u_i \rangle \tag{1}$$

$$\psi = \frac{1}{\Omega}\int_\Omega \phi \, d\,\Omega \equiv \langle \phi \rangle \tag{2}$$

  where Ω denotes the domain occupied by the UC and its volume.
- *Assumption 2:* The effective material properties obtained from the micromechanical analysis of the UC are independent of the geometry, the boundary conditions, and loading conditions of the macroscopic structure, which means that effective properties are assumed to be the intrinsic properties of the material when viewed macroscopically.

Note that these assumptions are not restrictive. The mathematical meaning of the first assumption is that the exact solutions of the field variables can be integrated over the domain of UC, which is true almost all the time. The second assumption implies that we will neglect the size effects of the material properties in the macroscopic analysis, which is an assumption often made in the conventional continuum mechanics. Of course, the micromechanical analysis of the UC is only needed and appropriate if $\eta = h/l \ll 1$, with h as the characteristic size of the UC and l as the characteristic wavelength of the deformation of the structure. Other assumptions such as particular geometry shape and arrangement of the constituents, specific boundary conditions applied to the UC, and prescribed relations between local fields and global fields are not necessary for the present study.

This new micromechanical modeling approach has been successfully used to predict the effective thermoelastic properties including elastic constants, specific heats, and coefficients of thermal expansions, and effective thermal conductivity and associated local fields (Yu and Tang, 2007a,b; Tang and Yu, 2007a). It is also applied to accurately predict the initial yielding surface and elastoplastic behavior of metal matrix composites (Tang and Yu, 2007b).

2. Piezoelectricity and piezoelectric composites

The elastic and the dielectric responses are coupled in piezoelectric materials where the mechanical variables of stress, and strain are related to each other as well as to the electric variables of electric field and electric displacement. The coupling between mechanical and electric fields is described by piezoelectric coefficients. Using the

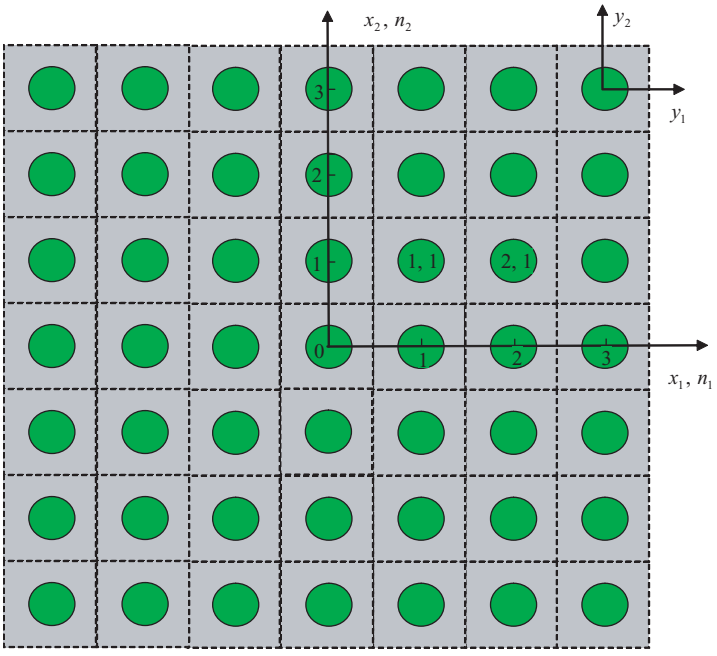

Fig. 1. Coordinate systems for heterogenous materials (only two-dimensional (2D) UC is drawn for clarity).

conventional indicial notation, the linear coupled constitutive equations are expressed as

$$\begin{aligned}\sigma_{ij} &= C_{ijkl}\epsilon_{kl} - e_{ijk}E_k \\ T_i &= e_{ikl}\epsilon_{kl} + k_{ij}E_j\end{aligned} \tag{3}$$

where σ_{ij}, ϵ_{ij}, E_i and T_i are the stress tensor, strain tensor, electric field vector, and the electric displacement vector, respectively. C_{ijkl} denotes fourth-order elasticity tensor at constant electric field, k_{ij} is the second-order dielectric tensor at constant strain field, e_{ijk} is the third-order piezoelectric coupling tensor. To avoid the difficulty associated with heterogeneity, we can use the micromechanics approach to homogenize the material and obtain an effective constitutive model, such that

$$\begin{aligned}\bar{\sigma}_{ij} &= C^*_{ijkl}\bar{\epsilon}_{kl} - e^*_{ijk}\bar{E}_k \\ \bar{T}_i &= e^*_{ijk}\bar{\epsilon}_{jk} + k^*_{ij}\bar{E}_j\end{aligned} \tag{4}$$

where "over-bar" means variables used in the macroscopic analysis of homogenized materials, and superscripts "*" denote the effective properties whose calculation are determined by the micromechanics model one employs.

3. Theoretical formulation

VAMUCH formulation uses three coordinates systems: two cartesian coordinates $\mathbf{x} = (x_1, x_2, x_3)$ and $\mathbf{y}=(y_1,y_2,y_3)$, and an integer-valued coordinate $\mathbf{n} = (n_1, n_2, n_3)$ (see Fig. 1). We use x_i as the global coordinates to describe the macroscopic structure and y_i parallel to x_i as the local coordinates to describe the UC (Here and throughout the paper, Latin indices assume 1, 2, and 3 and repeated indices are summed over their range except where explicitly indicated). We choose the origin of the local coordinates y_i to be the geometric center of UC. For example, if the UC is a cube with dimensions as d_i, then $y_i \in [-\frac{d_i}{2}, \frac{d_i}{2}]$. To uniquely locate a UC in the heterogeneous material we also introduce integer coordinates n_i. The integer coordinates are related to the global coordinates in such a way that $n_i = x_i/d_i$ (no summation over i). It is emphasized although only square array is sketched in Fig. 1, the present theory has no such limitations.

As implied by Assumption 2, we can obtain the same effective properties from an imaginary, unbounded, and unloaded heterogeneous material with the same microstructure as the real, loaded, and bounded one. Hence we could derive the micromechanics model from an imaginary, unloaded, heterogeneous material which completely occupies the three-dimensional (3D) space $\mathscr{R}$ and composes of infinite many repeating UCs. For piezoelectric composites, the total electric enthalpy is equal to the summation of the electric enthalpy stored in all the UCs, which is

$$\Pi = \sum_{n=-\infty}^{\infty} \int_{\Omega} 2H \, \mathrm{d}\Omega \tag{5}$$

where $2H$ is twice the electric enthalpy, given by

$$2H = \epsilon^T D \epsilon \tag{6}$$

with

$$\epsilon = \lfloor \epsilon_{11}, 2\epsilon_{12}, \epsilon_{22}, 2\epsilon_{13}, 2\epsilon_{23}, \epsilon_{33}, E_1, E_2, E_3 \rfloor^T \tag{7}$$

containing both the 3D strain field ϵ_{ij} and the 3D electric field E_i, which are defined for a linear theory as

$$\epsilon_{ij}(\mathbf{n};\mathbf{y}) = \frac{1}{2}\left[\frac{\partial u_i(\mathbf{n};\mathbf{y})}{\partial y_j} + \frac{\partial u_j(\mathbf{n};\mathbf{y})}{\partial y_i}\right] \tag{8}$$

$$E_i(\mathbf{n};\mathbf{y}) = -\frac{\partial \phi(\mathbf{n};\mathbf{y})}{\partial y_i} \tag{9}$$

and D is a 9×9 matrix including the elastic, piezoelectric, and dielectric properties and is expressed as

$$D = \begin{bmatrix} \boldsymbol{C} & -\boldsymbol{e} \\ -\boldsymbol{e}^T & -\boldsymbol{k} \end{bmatrix} \tag{10}$$

In view of the fact that the infinite many UCs form a continuous heterogenous material, we need to enforce the continuity of the displacement field u_i and the electric potential field ϕ on the interface between adjacent UCs, which is

$$\begin{aligned} u_i(n_1,n_2,n_3;d_1/2,y_2,y_3) &= u_i(n_1+1,n_2,n_3;-d_1/2,y_2,y_3) \\ u_i(n_1,n_2,n_3;y_1,d_2/2,y_3) &= u_i(n_1,n_2+1,n_3;y_1,-d_2/2,y_3) \\ u_i(n_1,n_2,n_3;y_1,y_2,d_3/2) &= u_i(n_1,n_2,n_3+1;y_1,y_2,-d_3/2) \end{aligned} \tag{11}$$

$$\begin{aligned} \phi(n_1,n_2,n_3;d_1/2,y_2,y_3) &= \phi(n_1+1,n_2,n_3;-d_1/2,y_2,y_3) \\ \phi(n_1,n_2,n_3;y_1,d_2/2,y_3) &= \phi(n_1,n_2+1,n_3;y_1,-d_2/2,y_3) \\ \phi(n_1,n_2,n_3;y_1,y_2,d_3/2) &= \phi(n_1,n_2,n_3+1;y_1,y_2,-d_3/2) \end{aligned} \tag{12}$$

It is pointed out that the continuity of the traction and the electric displacement is guaranteed by the variational principle if the continuity of the displacement and the electric potential is satisfied. Of course, if the displacement and the electric potential are solved approximately using a numerical technique such as the finite element method (FEM), then the continuity of the traction and the electric displacement will only be satisfied approximately although the continuity of the displacement and the electric potential can be satisfied exactly through the same nodal values.

The exact solution of the present problem will minimize the summation of electric enthalpy in Eq. (5) under the constraints in Eqs. (1), (2), (11), and (12). Due to discrete integer arguments, the problem is very difficult to solve. To avoid the difficulty associated with discrete integer arguments, we can reformulate the problem, including Eqs. (5), (8), (9), (11) and (12), in terms of continuous functions using the idea of quasicontinuum (Kunin, 1982). The corresponding formulas are listed below

$$\Pi = \int_{\mathscr{R}} \langle \epsilon^T D \epsilon \rangle \mathrm{d}\mathscr{R} \tag{13}$$

$$\epsilon_{ij}(\mathbf{x};\mathbf{y}) = \frac{1}{2}\left[\frac{\partial u_i(\mathbf{x};\mathbf{y})}{\partial y_j} + \frac{\partial u_j(\mathbf{x};\mathbf{y})}{\partial y_i}\right] \equiv u_{(i|j)} \tag{14}$$

$$E_i(\mathbf{x};\mathbf{y}) = -\frac{\partial \phi(\mathbf{x};\mathbf{y})}{\partial y_i} \tag{15}$$

and

$$\begin{aligned} u_i(x_1,x_2,x_3;d_1/2,y_2,y_3) &= u_i(x_1+d_1,x_2,x_3;-d_1/2,y_2,y_3) \\ u_i(x_1,x_2,x_3;y_1,d_2/2,y_3) &= u_i(x_1,x_2+d_2,x_3;y_1,-d_2/2,y_3) \\ u_i(x_1,x_2,x_3;y_1,y_2,d_3/2) &= u_i(x_1,x_2,x_3+d_3;y_1,y_2,-d_3/2) \end{aligned} \tag{16}$$

$$\begin{aligned}\phi(x_1,x_2,x_3;d_1/2,y_2,y_3)&=\phi(x_1+d_1,x_2,x_3;-d_1/2,y_2,y_3)\\ \phi(x_1,x_2,x_3;y_1,d_2/2,y_3)&=\phi(x_1,x_2+d_2,x_3;y_1,-d_2/2,y_3)\\ \phi(x_1,x_2,x_3;y_1,y_2,d_3/2)&=\phi(x_1,x_2,x_3+d_3;y_1,y_2,-d_3/2)\end{aligned} \tag{17}$$

Introducing Lagrange multipliers, we can pose the variational statement of the micromechanical analysis of UC as a stationary value problem of the following functional:

$$\begin{aligned}J=\int_{\mathscr{R}}\{&\langle\epsilon^T D\epsilon\rangle+\lambda_i(\langle u_i\rangle-v_i)+\lambda(\langle\phi\rangle-\psi)\\&+\int_{S_1}\gamma_{i1}[u_i(x_j;d_1/2,y_2,y_3)\\&-u_i(x_j+\delta_{j1}d_1;-d_1/2,y_2,y_3)]\mathrm{d}S_1\\&+\int_{S_2}\gamma_{i2}[u_i(x_j;y_1,d_2/2,y_3)\\&-u_i(x_j+\delta_{j2}d_2;y_1,-d_2/2,y_3)]\mathrm{d}S_2\\&+\int_{S_3}\gamma_{i3}[u_i(x_j;y_1,y_2,d_3/2)\\&-u_i(x_j+\delta_{j3}d_3;y_1,y_2,-d_3/2)]\mathrm{d}S_3\\&+\int_{S_1}\beta_1[\phi(x_j;d_1/2,y_2,y_3)\\&-\phi(x_j+\delta_{j1}d_1;-d_1/2,y_2,y_3)]\mathrm{d}S_1\\&+\int_{S_2}\beta_2[\phi(x_j;y_1,d_2/2,y_3)\\&-\phi(x_j+\delta_{j2}d_2;y_1,-d_2/2,y_3)]\mathrm{d}S_2\\&+\int_{S_3}\beta_3[\phi(x_j;y_1,y_2,d_3/2)\\&-\phi(x_j+\delta_{j3}d_3;y_1,y_2,-d_3/2)]\mathrm{d}S_3\}\,\mathrm{d}\mathscr{R}\end{aligned} \tag{18}$$

where λ_i, λ, γ_{ij}, and β_i are Lagrange multipliers introduced to enforce the constraints in Eqs. (1), (2), (16) and (17), respectively, S_i are the surfaces with $n_i=1$, x_j represents the triplet of x_1,x_2,x_3, and δ_{ij} is the Kronecker delta. Following the general procedure of VAMUCH, we can obtain the following change of variables for u_i and ϕ:

$$u_i(\mathbf{x};\mathbf{y})=v_i(\mathbf{x})+y_j\frac{\partial v_i}{\partial x_j}+\chi_i(\mathbf{x};\mathbf{y}) \tag{19}$$

$$\phi(\mathbf{x};\mathbf{y})=\psi(\mathbf{x})+y_i\frac{\partial\psi}{\partial x_i}+\zeta(\mathbf{x};\mathbf{y}) \tag{20}$$

where χ_i and ζ are the fluctuation functions, satisfying the following constraints in view of Eqs. (1), (19), (2), (20) when the origin of the local coordinate system is chosen to be the center of UC:

$$\langle\chi_i\rangle=0 \tag{21}$$

$$\langle\zeta\rangle=0 \tag{22}$$

Substituting Eqs. (19) and (20) into Eq. (18), we obtain a stationary value problem defined over UC for χ_i and ζ according to the variational asymptotic method (Berdichevsky, 1977), such that

$$\begin{aligned}J_\Omega=&\langle\epsilon^T D\epsilon\rangle+\lambda_i\langle\chi_i\rangle+\lambda\langle\zeta\rangle+\sum_{j=1}^{3}\int_{S_j}\gamma_{ij}(\chi_i^{+j}-\chi_i^{-j})\,\mathrm{d}S_j\\&+\sum_{j=1}^{3}\int_{S_j}\beta_j(\zeta^{+j}-\zeta^{-j})\,\mathrm{d}S_j\end{aligned} \tag{23}$$

with

$$\chi_i^{+j}=\chi_i|_{y_j=d_j/2},\chi_i^{-j}=\chi_i|_{y_j=-d_j/2}\text{ for }j=1,2,3$$

$$\zeta^{+j}=\zeta|_{y_j=d_j/2},\zeta^{-j}=\zeta|_{y_j=-d_j/2}\text{ for }j=1,2,3$$

Matrix ϵ can be expressed as

$$\epsilon=\bar{\epsilon}+\epsilon_1 \tag{24}$$

with

$$\begin{aligned}\bar{\epsilon}=\Big\lfloor&\frac{\partial v_1}{\partial x_1},\frac{\partial v_1}{\partial x_2}+\frac{\partial v_2}{\partial x_1},\frac{\partial v_2}{\partial x_2},\frac{\partial v_1}{\partial x_3}+\frac{\partial v_3}{\partial x_1},\frac{\partial v_2}{\partial x_3}\\&+\frac{\partial v_3}{\partial x_2},\frac{\partial v_3}{\partial x_3},-\frac{\partial\psi}{\partial x_1}-\frac{\partial\psi}{\partial x_2},-\frac{\partial\psi}{\partial x_3}\Big\rfloor^T\end{aligned} \tag{25}$$

which will be shown later to be the global variables containing both the strain field and the electric field for the material with homogenized effective material properties, and

$$\begin{aligned}\epsilon_1=\Big\lfloor&\frac{\partial\chi_1}{\partial y_1},\frac{\partial\chi_1}{\partial y_2}+\frac{\partial\chi_2}{\partial y_1},\frac{\partial\chi_2}{\partial y_2},\frac{\partial\chi_1}{\partial y_3}\\&+\frac{\partial\chi_3}{\partial y_1},\frac{\partial\chi_2}{\partial y_3}+\frac{\partial\chi_3}{\partial y_2},\frac{\partial\chi_3}{\partial y_3},-\frac{\partial\zeta}{\partial y_1},-\frac{\partial\zeta}{\partial y_2},-\frac{\partial\zeta}{\partial y_3}\Big\rfloor^T\end{aligned} \tag{26}$$

The functional J_Ω in Eq. (23) forms the backbone of the present theory. This variational statement can be solved analytically for very simple cases such as binary composites, however, for general cases we need to use numerical techniques such as FEM to seek numerical solutions.

4. Finite element implementation

It is possible to formulate the FEM solution based on Eq. (23), however, it is not the most convenient and efficient way because Lagrange multipliers will increase the number of unknowns. To this end, we can reformulate the variational statement in Eq. (23) as the minimum value of the following functional

$$\Pi_\Omega=\frac{1}{\Omega}\int_\Omega\epsilon^T D\epsilon\,\mathrm{d}\Omega \tag{27}$$

under the following constraints

$$\chi_i^{+j}=\chi_i^{-j}\text{ and }\zeta^{+j}=\zeta^{-j}\text{ for }j=1,2,3 \tag{28}$$

It is noted here that the constraints in Eq. (28) are the commonly assumed periodic boundary conditions. However, here both Eqs. (27) and (28) are direct consequence of Eq. (23), that is the periodic boundary conditions are derived from the theory instead of assumed a priori. The constraint in Eqs. (21) and (22) does not affect the minimum values of Π_Ω but help uniquely determine χ_i and ζ. In practice, we can constrain the fluctuation function at an arbitrary node to be zero and later use this constraint to recover the unique fluctuation function. It is fine to use penalty function method to introduce the constraints in Eq. (28). However, this method introduces additional approximation and the robustness of the solution depends on the choice of large penalty numbers. Instead, we make the nodes on the positive boundary surface (i.e., $y_i=d_i/2$) slave to the nodes on the opposite negative boundary surface (i.e., $y_i=-d_i/2$). By assembling all the

independent active degrees of freedom (DOFs), we can implicitly and exactly incorporate the constraints in Eq. (28).

Introduce the following matrix notation

$$\epsilon_1 == \begin{bmatrix} \frac{\partial}{\partial y_1} & 0 & 0 & 0 \\ \frac{\partial}{\partial y_2} & \frac{\partial}{\partial y_1} & 0 & 0 \\ 0 & \frac{\partial}{\partial y_2} & 0 & 0 \\ \frac{\partial}{\partial y_3} & 0 & \frac{\partial}{\partial y_1} & 0 \\ 0 & \frac{\partial}{\partial y_3} & \frac{\partial}{\partial y_2} & 0 \\ 0 & 0 & \frac{\partial}{\partial y_3} & 0 \\ 0 & 0 & 0 & -\frac{\partial}{\partial y_1} \\ 0 & 0 & 0 & -\frac{\partial}{\partial y_2} \\ 0 & 0 & 0 & -\frac{\partial}{\partial y_3} \end{bmatrix} \begin{bmatrix} \chi_1 \\ \chi_2 \\ \chi_3 \\ \zeta \end{bmatrix} \equiv \Gamma_h \chi \tag{29}$$

where Γ_h is an operator matrix. If we discretize χ using the finite elements as

$$\chi(x_i; y_i) = S(y_i)\mathscr{X}(x_i) \tag{30}$$

where S representing the shape functions and $\mathscr{X}$ a column matrix of the nodal values of both the mechanical and electric fluctuation functions. Substituting Eqs. (29) and (30) into Eq. (27), we obtain a discretized version of the functional as

$$\Pi_\Omega = \frac{1}{\Omega}(\mathscr{X}^T E \mathscr{X} + 2\mathscr{X}^T D_{h\epsilon}\bar{\epsilon} + \bar{\epsilon}^T D_{\epsilon\epsilon}\bar{\epsilon}) \tag{31}$$

where

$$\begin{aligned} E &= \int_\Omega (\Gamma_h S)^T D (\Gamma_h S)\, \mathrm{d}\Omega \\ D_{h\epsilon} &= \int_\Omega (\Gamma_h S)^T D\, \mathrm{d}\Omega \\ D_{\epsilon\epsilon} &= \int_\Omega D\, \mathrm{d}\Omega \end{aligned} \tag{32}$$

Minimizing Π_Ω in Eq. (31), we obtain the following linear system

$$E\mathscr{X} = -D_{h\epsilon}\bar{\epsilon} \tag{33}$$

It is clear from Eq. (33) that the fluctuation function $\mathscr{X}$ is linearly proportional to $\bar{\epsilon}$, which means the solution can be written symbolically as

$$\mathscr{X} = \mathscr{X}_0\bar{\epsilon} \tag{34}$$

Substituting Eq. (34) into Eq. (31), we can calculate the electric enthalpy of the UC as

$$\Pi_\Omega = \frac{1}{\Omega}\bar{\epsilon}^T(\mathscr{X}_0^T D_{h\epsilon} + D_{\epsilon\epsilon})\bar{\epsilon} \equiv \bar{\epsilon}^T \overline{D}\bar{\epsilon} \tag{35}$$

It can be seen that $\overline{D}$ in Eq. (35) is the effective piezoelectric material properties which can be expressed using a 9×9 matrix as

$$\overline{D} = \begin{bmatrix} \mathbf{C}^* & -\boldsymbol{e}^* \\ -\boldsymbol{e}^{*T} & -\boldsymbol{k}^* \end{bmatrix} \tag{36}$$

and $\bar{\epsilon}$ is a column matrix containing both the global strains and global electric fields.

If the local fields within UC are of interest, one can recover those fields, such as local displacements, electric potential, stresses, and electric displacements, in terms of the macroscopic behavior including the global displacements v_i, the global electric potential ψ, the global strain and electric field $\bar{\epsilon}$, and the fluctuation function χ. First, we need to uniquely determine the fluctuation functions. Considering the fact that we fixed an arbitrary node and made nodes on the positive boundary surfaces slave to the corresponding negative boundary surfaces, we need to construct a new array $\widetilde{\mathscr{X}_0}$ from $\mathscr{X}_0$ by assigning the values for slave nodes according to the corresponding active nodes and assign zero to the fixed node. Obviously, $\widetilde{\mathscr{X}_0}$ still yield the minimum value of Π_Ω in Eq. (27) under constraints in Eq. (28). However, $\widetilde{\mathscr{X}_0}$ may not satisfy Eqs. (21) and (22). The real solution, denoted as $\overline{\mathscr{X}_0}$ can be found trivially by adding a constant corresponding to each DOF to each node so that Eqs. (21) and (22) are satisfied.

After having determined the fluctuation functions uniquely, we can recover the local displacements and electric potential using Eqs. (19) and (20) as

$$\begin{Bmatrix} u_1 \\ u_2 \\ u_3 \\ \phi \end{Bmatrix} = \begin{Bmatrix} v_1 \\ v_2 \\ v_3 \\ \psi \end{Bmatrix} + \begin{bmatrix} \frac{\partial v_1}{\partial x_1} & \frac{\partial v_1}{\partial x_2} & \frac{\partial v_1}{\partial x_3} \\ \frac{\partial v_2}{\partial x_1} & \frac{\partial v_2}{\partial x_2} & \frac{\partial v_2}{\partial x_3} \\ \frac{\partial v_3}{\partial x_1} & \frac{\partial v_3}{\partial x_2} & \frac{\partial v_3}{\partial x_3} \\ \frac{\partial \psi}{\partial x_1} & \frac{\partial \psi}{\partial x_2} & \frac{\partial \psi}{\partial x_3} \end{bmatrix} \begin{Bmatrix} y_1 \\ y_2 \\ y_3 \end{Bmatrix} + \overline{S\mathscr{X}} \tag{37}$$

Here $\overline{S}$ is different from S due to the recovery of slave nodes and the constrained node. The local strain field and electric field can be recovered using Eqs. (14), (15), (19), (20) and (29) as

$$\epsilon = \bar{\epsilon} + \Gamma_h \overline{S\mathscr{X}} \tag{38}$$

Finally, the local stress and electric displacement field can be recovered straightforwardly using the 3D constitutive relations for the constituent material as

$$\sigma = D\epsilon \tag{39}$$

with σ as a column matrix containing both 3D stresses and electric displacements such that

$$\sigma = \lfloor \sigma_{11}, \sigma_{12}, \sigma_{22}, \sigma_{13}, \sigma_{23}, \sigma_{33}, -T_1, -T_2, -T_3 \rfloor^T \tag{40}$$

We have implemented this formulation in the computer program VAMUCH. To demonstrate the application, accuracy, and efficiency of this theory and the companion code,

Table 1
Material properties of the composite constituents (PZT-7A, Epoxy, SiC, LaRC-SI, and PVDF)

	PZT-7A	Epoxy	SiC	LaRC-SI	PVDF
C_{11}	131.39	8.0	483.7	8.1	1.2
C_{12}	87.712	4.4	99.1	5.4	1.0
C_{23}	83.237	4.4	99.1	5.4	1.9
C_{22}	154.837	8.0	483.7	8.1	3.8
C_{44}	35.8	1.8	192.3	1.4	0.7
C_{55}	25.696	1.8	192.3	1.4	0.9
C_{66}	25.696	1.8	192.3	1.4	0.9
e_{11}	9.52183	–	–	–	−0.027
e_{21}	−2.12058	–	–	–	0.024
e_{31}	−2.12058	–	–	–	0.001
e_{51}	9.34959	–	–	–	0.000
k_{11}	2.079	0.0372	0.085	0.025	0.067
k_{22}	4.065	0.0372	0.085	0.025	0.065
k_{33}	4.065	0.0372	0.085	0.025	0.082

we will analyze several examples using VAMUCH in the next section.

5. Numerical examples

VAMUCH provides a unified analysis for general 1D, 2D, or 3D UCs. First, the same code VAMUCH can be used to homogenize binary composites (modeled using 1D UCs), fiber reinforced composites (modeled using 2D UCs), and particle reinforced composites (modeled using 3D UCs). Second, VAMUCH can reproduce the results for lower-dimensional UCs using higher-dimensional UCs. That is, VAMUCH predicts the same results for binary composites using 1D, 2D or 3D UCs, and for fiber reinforced composites using 2D or 3D UCs.

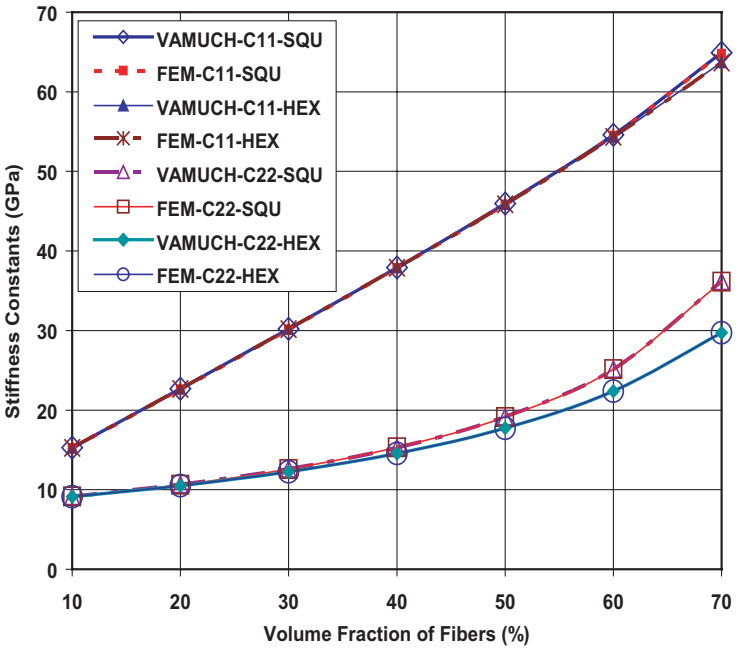

Fig. 2. Effective stiffness constants C_{11} and C_{22}.

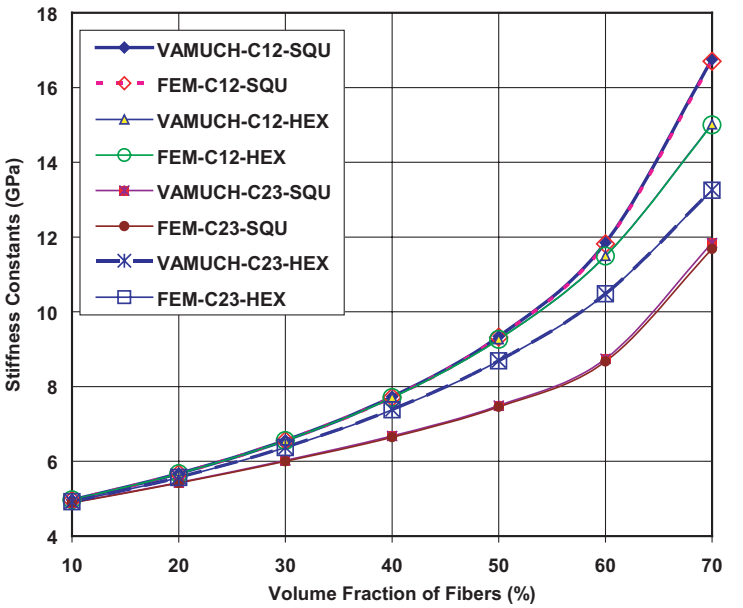

Fig. 3. Effective stiffness constants C_{12} and C_{23}.

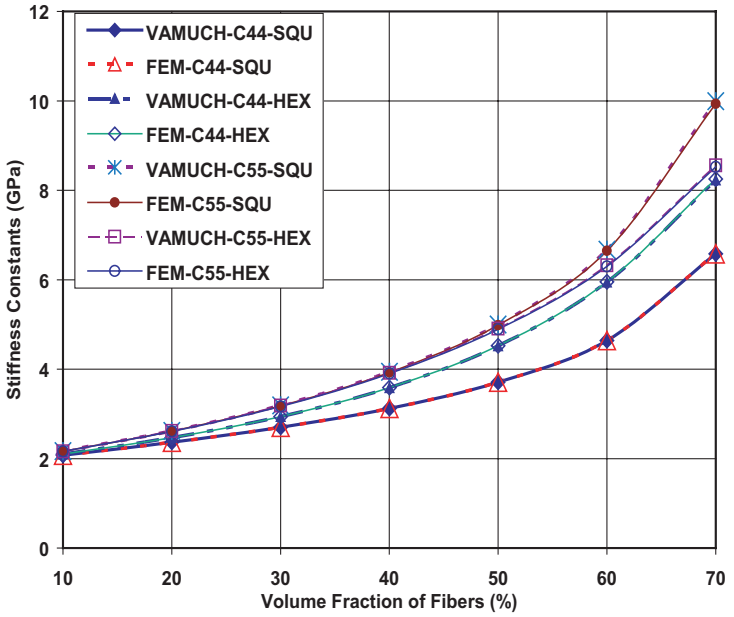

Fig. 4. Effective stiffness constants C_{44} and C_{55}.

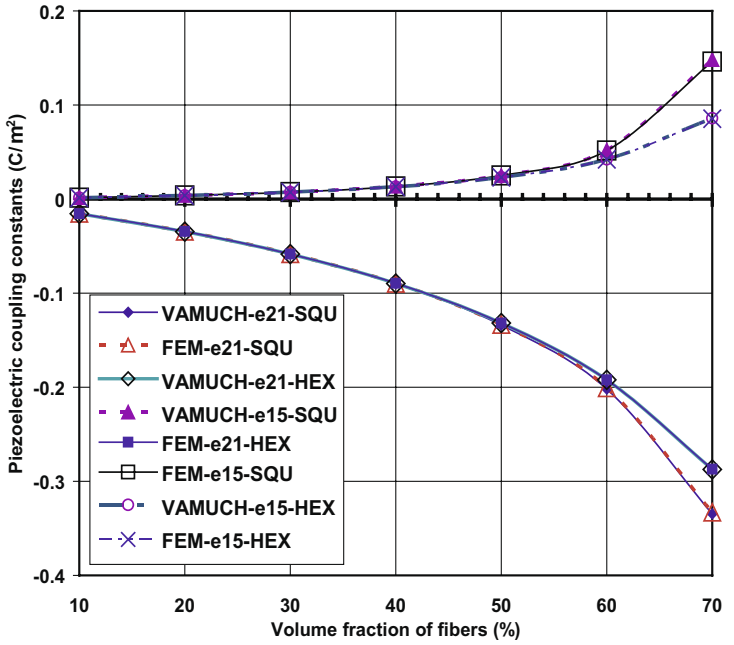

Fig. 5. Effective electric coupling constants.

In this section, several examples will be used to demonstrate the accuracy of VAMUCH for predicting the effective properties and calculating the local stress and electric displacement fields within UC.

5.1. Predict effective properties of composites

At first the piezoelectric composite considered is composed of piezoceramic (PZT) fibers embedded in soft non-piezoelectric materials (epoxy) in which the fibers are of circular shape. The epoxy matrix is isotropic while the fibers are transversely isotropic. The material properties of both constituents are taken from Pettermann and Suresh (2000) and shown in Table 1. The units of the elastic constants, piezoelectric constants, and dielectric constants are given in GPa, Cm^{-2}, and nC V^{-1} m^{-1}, respectively. For transversely isotropic piezoelectric materials, there are 11 independent coefficients remained in the total material

matrix and the matrix form of constitutive equation can be written as

$$\begin{Bmatrix} \sigma_{11} \\ \sigma_{12} \\ \sigma_{22} \\ \sigma_{13} \\ \sigma_{23} \\ \sigma_{33} \\ -T_1 \\ -T_2 \\ -T_3 \end{Bmatrix} = \begin{bmatrix} C_{11} & 0 & C_{12} & 0 & 0 & C_{12} & -e_{11} & 0 & 0 \\ 0 & C_{66} & 0 & 0 & 0 & 0 & 0 & -e_{51} & 0 \\ C_{12} & 0 & C_{22} & 0 & 0 & C_{23} & -e_{21} & 0 & 0 \\ 0 & 0 & 0 & C_{55} & 0 & 0 & 0 & 0 & -e_{51} \\ 0 & 0 & 0 & 0 & C_{44} & 0 & 0 & 0 & 0 \\ C_{12} & 0 & C_{23} & 0 & 0 & C_{22} & -e_{21} & 0 & 0 \\ -e_{11} & 0 & -e_{21} & 0 & 0 & -e_{21} & -k_{11} & 0 & 0 \\ 0 & -e_{51} & 0 & 0 & 0 & 0 & 0 & -k_{22} & 0 \\ 0 & 0 & 0 & -e_{51} & 0 & 0 & 0 & 0 & -k_{22} \end{bmatrix} \begin{Bmatrix} \epsilon_{11} \\ \epsilon_{12} \\ \epsilon_{22} \\ \epsilon_{13} \\ \epsilon_{23} \\ \epsilon_{33} \\ E_1 \\ E_2 \\ E_3 \end{Bmatrix} \tag{41}$$

All effective coefficients were calculated for the volume fraction of fibers in a range between 0.1 and 0.7 using VAMUCH and ANSYS, a commercial finite element package capable of multiphysics simulation. For ANSYS calculation, we need to use a three-dimensional unit cell, which is meshed with 8-noded piezoelectric brick elements (Solid5) with area element size 0.05. However, for VAMUCH calculation, we only need a two-dimensional unit cell, which is meshed with 4-noded quadrilateral elements with the same element size. Both meshes provide converged results for the effective properties. The ANSYS FEM model was set up following the procedure described in Berger et al.

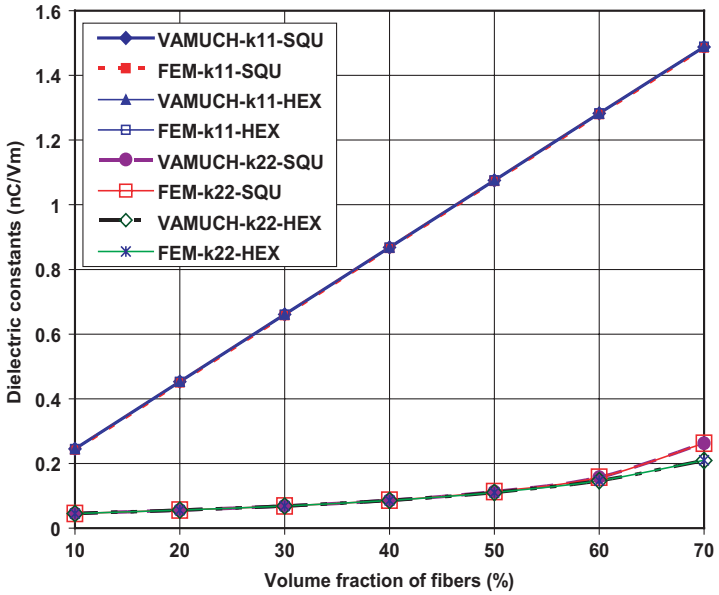

Fig. 6. Effective dielectric constants.

Table 2
Comparison of the effective properties for 60% volume fraction of fibers

	VAMUCH	Berger	Pettermann	BL	HS
C_{11}^{effD} (GPa)	86.982	86.982	86.98	76.1/87.0	79.0/87.8
C_{12}^{effD} (GPa)	10.630	10.631	10.64	8.89/12.3	6.12/16.5
C_{22}^{effD} (GPa)	25.322	25.322	25.42	25.2/25.5	24.9/28.7
C_{23}^{effD} (GPa)	7.931	7.930	7.86	7.72/8.15	5.00/12.0
C_{44}^{effD} (GPa)	4.39	4.39	4.41	4.39/4.41	4.37/4.92
C_{55}^{effD} (GPa)	6.481	6.477	6.51	6.45/6.52	6.40/7.67
β_{11}^{eff} (GVm/C)	0.780	0.780	0.780	0.730/0.844	0.742/0.951
β_{22}^{eff} (GVm/C)	6.614	6.60	6.572	6.57/6.66	2.54/6.73
h_{11}^{eff} (GV/m)	5.039	5.039	5.037	3.91/5.42	3.63/5.85
h_{21}^{eff} (GV/m)	−0.1524	−0.1524	−0.153	−0.337/0.024	−1.03/0.719
h_{51}^{eff} (GV/m)	0.3068	0.3063	0.311	0.229/0.384	−1.92/2.67

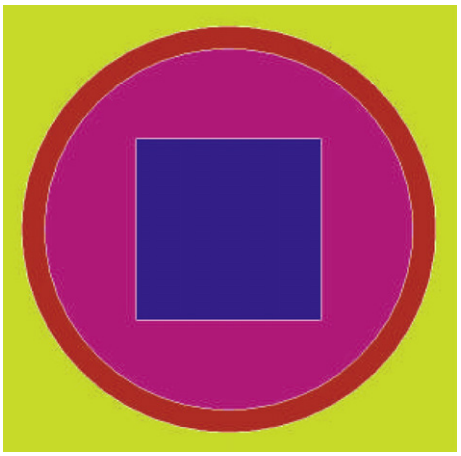

Fig. 7. Piezoelectric composite with a complex microstructure.

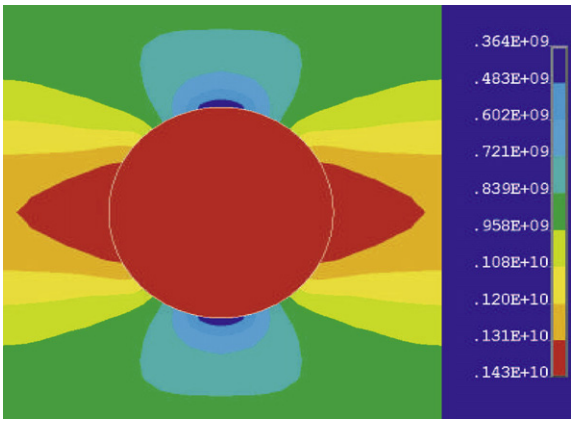

Fig. 8. Contour plot of σ_{22} (Pa) within UC.

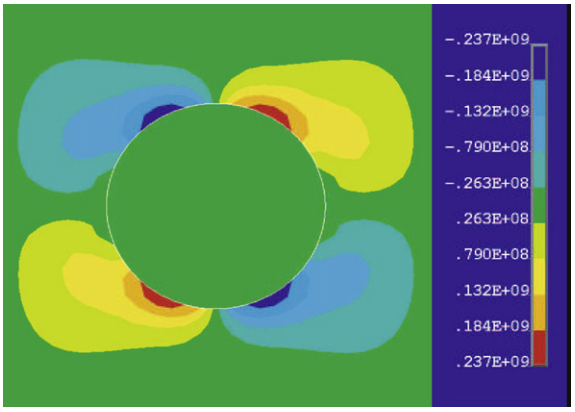

Fig. 9. Contour plot of σ_{23} (Pa) within UC.

(2006). The results of different approaches were evaluated for composites with periodic square (SQU) or periodic hexagonal (HEX) piezoelectric fiber arrangements. The effective coefficients of composites are shown in Figs. 2–6. We found out that the predictions of all effective coefficients from VAMUCH have excellent agreement with those using ANSYS following Berger et al. (2006).

To provide a more extensive validation for VAMUCH, we considered a composite body reinforced by parallel square fibers with a square arrangement, which is the same example as in Bisegna and Luciano (1997). The matrix and the fibers are isotropic epoxy polymer and piezoelectric ceramic PZT-7A, respectively. The volume fraction of fibers is 60%. For ANSYS calculation, we use 8-noded piezoelectric brick elements (Solid5) with area element size 0.05 and for VAMUCH calculation, we use 8-noded quadrilateral element with the same element size. Mesh refinements are also applied at the corner for convergence of the results. To facilitate the comparison, the effective coefficients calculated by VAMUCH are transformed according to the following formulas as listed in Berger et al. (2006):

$$
\begin{aligned}
&\beta_{11}^{\mathrm{eff}} = 1/\epsilon_{11}^{\mathrm{eff}} && \beta_{22}^{\mathrm{eff}} = 1/\epsilon_{22}^{\mathrm{eff}} \\
&C_{11}^{\mathrm{effD}} = C_{11}^{\mathrm{eff}} + (e_{11}^{\mathrm{eff}})^2\beta_{11}^{\mathrm{eff}} && C_{12}^{\mathrm{effD}} = C_{12}^{\mathrm{eff}} + e_{21}^{\mathrm{eff}} e_{11}^{\mathrm{eff}}\beta_{11}^{\mathrm{eff}} \\
&C_{22}^{\mathrm{effD}} = C_{22}^{\mathrm{eff}} + (e_{21}^{\mathrm{eff}})^2\beta_{11}^{\mathrm{eff}} && C_{23}^{\mathrm{effD}} = C_{23}^{\mathrm{eff}} + (e_{21}^{\mathrm{eff}})^2\beta_{11}^{\mathrm{eff}} \\
&C_{44}^{\mathrm{effD}} = C_{44}^{\mathrm{eff}} && C_{55}^{\mathrm{effD}} = C_{55}^{\mathrm{eff}} + (e_{51}^{\mathrm{eff}})^2\beta_{11}^{\mathrm{eff}} \\
&h_{11}^{\mathrm{effD}} = e_{11}^{\mathrm{eff}}\beta_{11}^{\mathrm{eff}} && h_{21}^{\mathrm{effD}} = e_{21}^{\mathrm{eff}}\beta_{11}^{\mathrm{eff}} \\
&h_{51}^{\mathrm{effD}} = e_{51}^{\mathrm{eff}}\beta_{22}^{\mathrm{eff}} &&
\end{aligned}
\tag{42}
$$

In Table 2, VAMUCH results are compared with ANSYS following the micromechanical analysis of Berger et al. (2006) (denoted as Berger), the results in Pettermann and Suresh (2000) (denoted as Pettermann), Bisegna–Luciano bounds in Bisegna and Luciano (1997) (denoted as BL), and Hashin–Shtrikman bounds for piezoelectric materials derived in Bisegna and Luciano (1997) (denoted as HS). From Table 2 one can observe that the predictions of VAMUCH agree very well with those of FEM-based micromechanical analyses (Pettermann and Suresh, 2000; Berger et al., 2006) and nicely fall in between the tightest BL bounds.

To further demonstrate the reliability and accuracy of present model for more realistic heterogeneous materials, we choose a more complex microstructure as shown in Fig. 7. There are four different materials within one UC. The reinforcements are PZT-7A square fiber and a thin-wall circular SiC frame around the square fiber. The matrix

Table 3
Effective coefficients of piezoelectric composite with a complex microstructure

	C_{11}^{eff} (GPa)	C_{12}^{eff} (GPa)	C_{23}^{eff} (GPa)	C_{22}^{eff} (GPa)	C_{44}^{eff} (GPa)	C_{55}^{eff} (GPa)
VAMUCH	75.51	3.33	5.173	10.916	1.871	3.86
ANSYS	75.51	3.33	5.167	10.920	1.871	3.82
	e_{11}^{eff} (C/m^2)	e_{21}^{eff} (C/m^2)	e_{51}^{eff} (C/m^2)	k_{11}^{eff} (nC/Vm)	k_{22}^{eff} (nC/Vm)	k_{33}^{eff} (nC/Vm)
VAMUCH	1.7387	0.009275	0.000735	0.3827	0.06011	0.06555
ANSYS	1.7387	0.009291	0.000753	0.3827	0.06013	0.06558

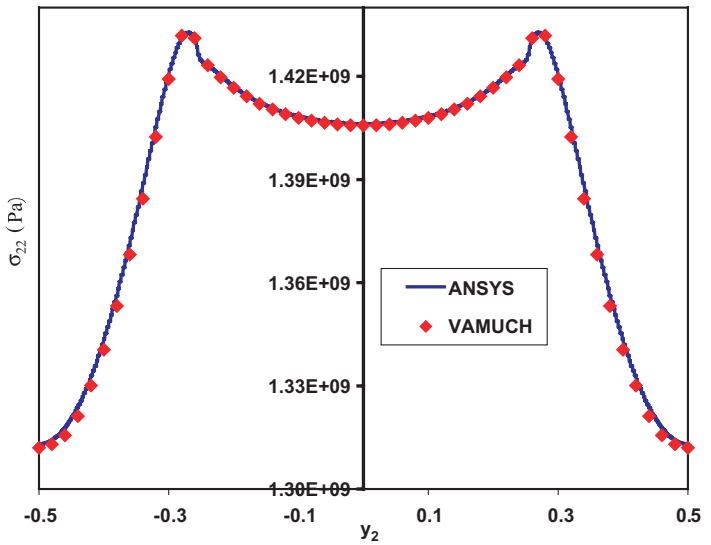

Fig. 10. Comparison of normal stress σ_{22} distribution along $y_3 = 0$.

between reinforcements is LaRC-SI, while the matrix outside thin-wall frame is PVDF. The material properties of the four constituents are shown in Table 1. There are no analytical solutions for this kind of microstructure. Here, we use ANSYS to calculate all the effective properties following the approach described in Berger et al. (2006). Table 3 lists the effective properties predicted by VAMUCH and ANSYS. Both methods produce almost identical results.

5.2. Predict local fields

VAMUCH can accurately recover the local stresses and electric displacement distribution within the UC. In this study, we will use the direct multiphysics simulation in ANSYS as benchmark to verify the prediction of VAMUCH. The first example is PZT-7A/epoxy fiber reinforced composites with fiber volume fraction as 0.2. The boundary condi-

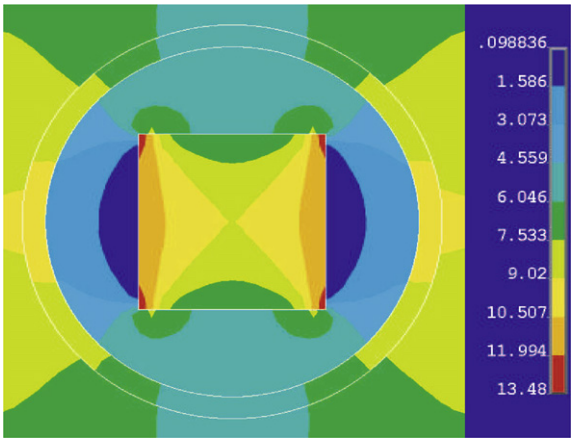

Fig. 12. Contour plot of electric flux density T_3 (nC/Vm) in a piezoelectric composite with complex microstructure.

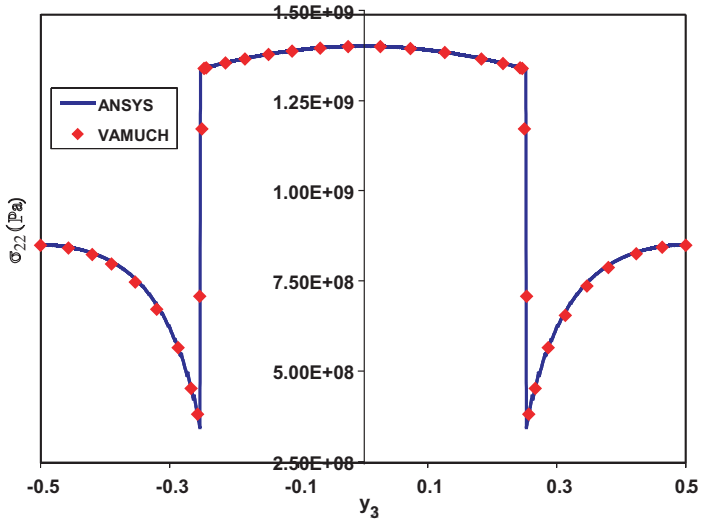

Fig. 11. Comparison of normal stress σ_{22} distribution along $y_2 = 0$.

tions applied to the UC are $\epsilon_{22} = 1.0\%$ and $E_2 = 100$ V/m and all other mechanical strains and gradients of electric potential are set to zero. Due to the difference of material properties of two constituents, the distribution of local stresses is not uniform within the UC. Figs. 8 and 9 show the contour plots of the distributions of σ_{22} and σ_{23}. All sudden changes of local stresses at the interface between fibers and matrix are well captured by VAMUCH. For quantitative comparison, we also plot σ_{22} predicted by VAMUCH and the direct multiphysics simulation of ANSYS along the lines $y_3 = 0$ and $y_2 = 0$ in Figs. 10 and 11, respectively. It is obvious that the predictions of VAMUCH have excellent agreement with those of ANSYS.

The second example is the composite with complex microstructure as shown in Fig. 7. The mechanical strains on all surfaces of UC are constrained. The contours of local electric displacement distribution T_3 and T_2 resulting from 100 V/m in the y_3 direction predicted by VAMUCH is shown in Figs. 12 and 13. For a quantitative comparison, we also plot the local electric displacement distribution T_3 along $y_3 = 0$ predicted by VAMUCH and ANSYS as shown in Fig. 14. It can be observed that there is excellent agreement between these two sets of results.

In the aforementioned two examples, the contour plots of ANSYS are not shown because they are indistinguishable

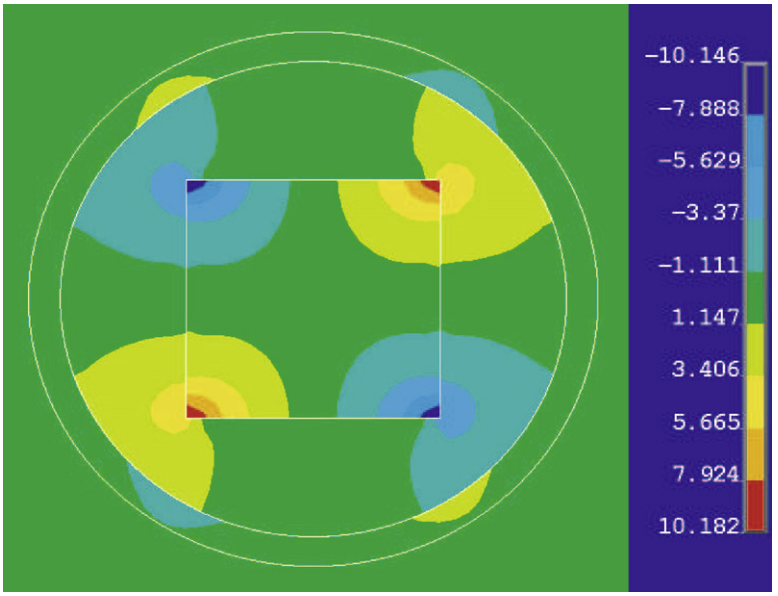

Fig. 13. Contour plot of electric flux density T_2 (nC/Vm) in a piezoelectric composite with complex microstructure.

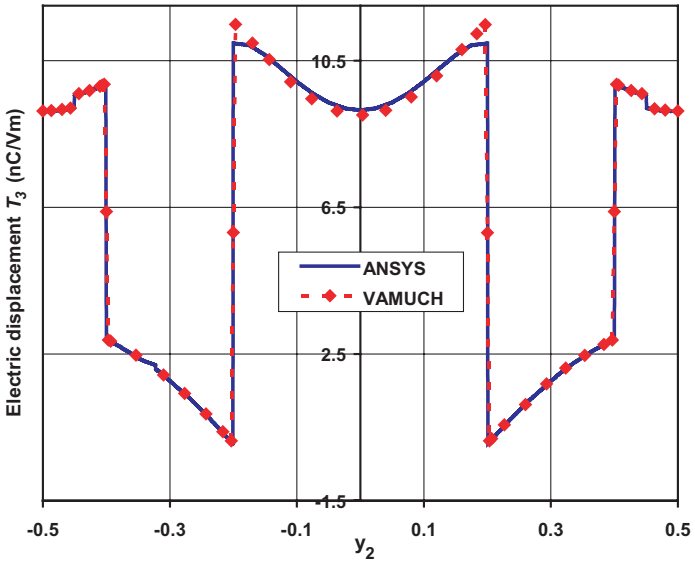

Fig. 14. Electric flux density T_3 distribution along $y_3 = 0$ in a piezoelectric composite with complex microstructure.

from those of VAMUCH. It is emphasized here that ANSYS results are obtained through the direct multiphysics simulation of the unit cell using piezoelectric elements under specified loading without using a micromechanics approach to obtain the effective properties first, while VAMUCH calculates the effective material properties first and use these effective properties to carry out a macroscopic analysis of the homogenized microstructure to obtain the global fields and then recover the local fields within the original heterogeneous microstructure.

6. Conclusion

The variational asymptotic method for unit cell homogenization (VAMUCH) has been applied to construct a micromechanics model for predicting the effective properties and the local fields of piezoelectric composites. In comparison to existing models, the present model has the following unique features:

(1) It adopts the variational asymptotic method as its mathematical foundation. It invokes only essential assumptions inherent in the concept of micromechanics.
(2) It has an inherent variational nature and its numerical implementation is shown to be straightforward.
(3) It handles 1D/2D/3D unit cells uniformly. The dimensionality of the problem is determined by the periodicity of the unit cell.

The present theory is implemented in the computer program, VAMUCH. Numerous examples have clearly demonstrated its application and accuracy as a general-purpose micromechanical analysis tool. Although for the examples we have studied, VAMUCH results are almost identical to the results obtained by some FEM-based micromechanics analysis (Pettermann and Suresh, 2000; Berger et al., 2006), VAMUCH has the following advantages:

(1) VAMUCH can obtain the complete set of material properties within one analysis, which is more efficient than those approaches requiring multiple runs under different boundary and load conditions. Furthermore, it is not a trivial issue to apply the right boundary conditions to obtain a correct FEM-based micromechanical analysis.
(2) VAMUCH calculates effective properties and local fields directly with the same accuracy as the fluctuation functions. No postprocessing calculations which introduces more approximations, such as averaging stress and electric displacement field, are needed, which are indispensable for FEM-based micromechanical analysis.
(3) VAMUCH can deal with general anisotropy for effective materials which means VAMUCH can calculate 21 constants for the effective elastic constants, 18 constants for the effective piezoelectric constants, 6 for the effective dielectric constants, while FEM-based micromechanical analyses have difficulties to predict effective material having constants more than orthotropic materials.

Acknowledgements

The present work is supported, in part, by the National Science Foundation under Grant DMI-0522908 and the State of Utah Community/University Research Initiative Grant. The views and conclusions contained herein are those of the authors and should not be interpreted as necessarily representing the official policies or endorsement, either expressed or implied, of the funding agencies. The authors want to sincerely thank Dr. Harald Berger from Otto-von-Guericke-University of Magdeburg, Germany, for technical discussions and kindly providing the ANSYS macro files and the data of effective properties of PZT-7A fiber reinforced composites.

References

Banno, H., 1983. Recent developments of piezoelectric ceramic products and composites of synthetic rubber and piezoelectric ceramic particles. Ferroelectrics 50, 329–338.
Benveniste, Y., 1987. A new approach to the application of Mori–Tanaka's theory in composite materials. Mechanics of Materials 6, 147–157.
Benveniste, Y., 1992. The determination of the elastic and electric fields in a piezoelectric inhomogeneity. Journal of Applied Physics 72, 1086–1095.
Berdichevsky, V.L., 1977. On averaging of periodic systems. PMM 41 (6), 993–1006.
Berger, H., Kari, S., Gabbert, U., Rodriguez-Ramos, R., Bravo-Castillero, J., Guinovart-Diaz, R., Sabina, F., Maugin, G., 2006. Unit cell models of piezoelectric fiber composites for numerical and analytical calculation of effective properties. Smart Materials and Structures 15, 451–458.
Bisegna, P., Luciano, R., 1996. Variational bounds for the overall properties of piezoelectric composites. Journal of the Mechanics and Physics of Solids 44, 583–602.
Bisegna, P., Luciano, R., 1997. On methods for bounding the overall properties of periodic piezoelectic fibrous composites. Journal of the Mechanics and Physics of Solids 45, 1329–1356.
Budiansky, B., 1965. On the elastic moduli of some heterogeneous materials. Journal of the Mechanics and Physics of Solids 13, 223–227.
Chan, H., Unsworth, J., 1989. Simple model for piezoelectric ceramic/polymer 1–3 composites used in ultrasonic transducer applications. IEEE Transactions on Ultrasonics, Ferroelectrics, and Frequency Control 36, 434–441.
Chen, T., 1993. Piezoelectric properties of multiphase fibrous composites: some theoretical results. Journal of the Mechanics and Physics of Solids 41, 1781–1794.
Dunn, M., Taya, M., 1993a. An analysis of piezoelectric composite materials containing ellipsoidal inhomogeneities. Proceedings of the Royal Society of London, Series A 443, 265–287.
Dunn, M., Taya, M., 1993b. Micromechanics predictions of the effective electroelastic moduli of piezoelectric composites. International Journal of Solids and Structures 30, 161–175.
Dunn, M., Taya, M., 1994. Micromechanical estimates of the overall thermoelectroelastic moduli of multiphase fibrous composites. International Journal of Solids and Structures 31, 3099–3111.
Eshelby, J., 1957. The determination of the elastic field of an ellipsoidal inclusion, and related problems. Proceedings of the Royal Society of London, Series A 241, 376–396.
Fakri, N., Azrar, L., El Bakkali, L., 2003. Electroelastic behavior modeling of piezoelectric composite materials containing spatiallly oritented reinforcements. International Journal of Solids and Structures 40, 361–384.
Gaudenzi, P., 1997. On the electromechanical response of active composite materials with piezoelectic inclusions. Computers and Structures 65, 157–168.
Hill, R., 1965. A self-consistent mechanics of composite materials. Journal of the Mechanics and Physics of Solids 13, 213–222.

Huang, J., Kuo, W., 1996. Micromechanics determination of the effective properties of piezoelectric composites containing spatially oriented short fibers. Acta Materialia 44, 4889–4898.

Kunin, I., 1982. Theory of Elastic Media with Microstructure, vols. 1 and 2. Springer Verlag.

Lenglet, E., Hladky-Hennion, A., Debus, J., 2003. Numerical homogenization techniques applied to piezoelectric composites. Journal of the Acoustical Society of America 113, 826–833.

Li, J., Dunn, M., 2001. Variational bounds for the effective moduli of heterogeneous piezoelectric solids. Philosophical Magazine 81, 903–926.

Li, S., 2000. General unit cells for micromechanical analysis of unidirectional composites. Composites A 32, 815–826.

McLaughlin, R., 1977. A study of the differential scheme for composite materials. International Journal of Engineering Science 15, 237–244.

Mori, T., Tanaka, K., 1973. Average stress in matrix and average elastic energy of materials with misfitting inclusions. Acta Metallurgica 21, 571–574.

Newnham, R., Skinner, D., Cross, L., 1978. Connectivity and piezoelectri-pyroelectric composites. Materials Research Bulletin 13, 525–536.

Norris, A., 1985. A differential scheme for the effective moduli of composites. Mechanics of Materials 4, 1–16.

Odegard, G.M., 2004. Constitutive modeling of piezoelectric polymer composites. Acta Materialia 52 (18), 5315–5330.

Pastor, J., 1997. Homogenization of linear piezoelectric media. Mechanics Research Communications 24, 145–150.

Pettermann, H., Suresh, S., 2000. A comprehensive unit cell model: A study of coupled effects in piezoelectric 1–3 composites. International Journal of Solids and Structures 37, 5447–5464.

Poizat, C., Sester, M., 1999. Effective properties of composites with embedded piezoelectric fibers. Computational Materials Science 16, 89–97.

Smith, W., Auld, B., 1991. Modeling 1–3 composites piezoelectrics: thickness-mode oscillations. IEEE Transactions on Ultrasonics, Ferroelectrics, and Frequency Control 38, 40–47.

Sun, H., Di, S., Zhang, N., Wu, C., 2001. Micromechanics of composite materials using multivariable finite element method and homogenization theory. International Journal of Solids and Structures 38, 3007–3020.

Tang, T., Yu, W., 2007a. A variational asymptotic micromechanics model for predicting conductivity of composite materials. Journal of Mechanics of Materials and Structures 2, 1813–1830.

Tang, T., Yu, W., Nov. 10–16 2007b. A variational asymptotic model for predicting initial yielding surface and elastoplastic behavior of metal matrix composite materials. In: Proceedings of the 2007 ASME International Mechanical Engineering Congress and Exposition. ASME, Seattle, Washington.

Wang, B., 1992. Three dimensional analysis of an ellipsoidal inclusion in a piezoelectic material. International Journal of Solids and Structures 29, 293–308.

Yu, W., Tang, T., 2007a. Variational asymptotic method for unit cell homogenization of periodically heterogeneous materials. International Journal of Solids and Structures 44, 3738–3755.

Yu, W., Tang, T., 2007b. A variational asymptotic micromechanics model for predicting thermoelastic properties of heterogeneous materials. International Journal of Solids and Structures 44, 7510–7525.